

# EXOMARS LOCOMOTION SUBSYSTEM ANALYTICAL TOOL DEVELOPMENT AND CORRELATION

ESA/ESTEC, NOORDWIJK, THE NETHERLANDS / 12 – 14 APRIL 2011

S. Michaud<sup>(1)</sup>, R. Krpoun<sup>(1)</sup>, S. Wismer<sup>(1)</sup>, D. Gloster<sup>(1)</sup>

<sup>(1)</sup>RUAG Space, Schaffhauserstrasse 580 CH-8052 Zurich (Switzerland),  
stephane.michaud@ruag.com

## ABSTRACT

*In order to assess rover performance and provide relevant inputs for sizing the mechanical and electrical elements of the ExoMars Locomotion Sub-system (LSS), an analytical tool that solves quasi-static equations in conjunction with wheel level test data was developed by RUAG Space on an R&D budget and using existing internally developed modules. This upgraded tool was correlated with test results from an ExoMars Breadboard level test programme on representative Martian soil and Lander platform. This analytical tool validation is limited by the availability of test data but can function as an alternative to more complex simulation applications in particular during the dimensioning phase. This paper presents the methodology used for developing the ExoMars LSS analytical tool, the evaluation of the test data used and the correlation activity performed in order to assess the overall prediction accuracy.*

## 1. INTRODUCTION

In the frame of the ESA ExoMars mission, it is intended that a rover will provide regional mobility (several kilometres) searching for traces of past and present life over its planned 218 sols of operation. The subsystem which handles the traction, obstacle traverse and slope climbing, enabling the rover vehicle to traverse the surface of Mars, is called the ExoMars Locomotion Subsystem (LSS) and is under development by RUAG Space.

In order to assess rover performance and provide relevant input for sizing the LSS mechanical and electrical elements, a rover and wheel level breadboard test program on representative Martian soil was conducted and is presented in [3]. However, due to the joint ESA/NASA mission, the possibility of landing a heavier rover, with additional instruments, emerged resulting in a modification of the overall rover mass from 250kg to 300kg. As a result, the previously generated test data is now partially obsolete and cannot be directly used for flowing down sub-system specifications. Upgrading the existing breadboard and repeating test campaign would require a significant time and cost. Therefore, in order to address this issue in the

short term, an analytical tool capable of computing accurately sizing loads and the peak power consumption for various ExoMars LSS configurations and mass distributions in conjunction with design rules was developed.

## 2. EXOMARS ROVER

### 2.1. Overview

The analytical tool development is focused on the ExoMars LSS configuration shown in Fig. 1. This passive suspension concept is based on 3 bogies mechanically connected to the rover body via passive joints allowing free rotation of the bogies [4]. The two lateral bogies are placed at the front of the rover and a transverse bogie is placed at the rear. On each bogie there are two legs featuring a deployment, steering and drive unit with a flexible wheel.

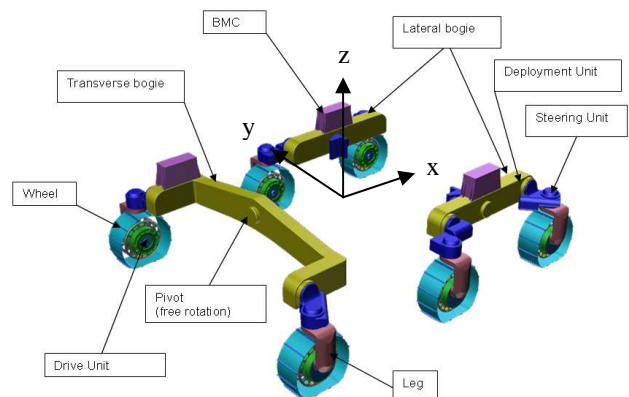


Figure 1. LSS Design Overview

### 2.2. LSS Breadboard Description

To achieve similar loads under Earth gravity as the currently foreseen 300 kg flight model on Mars, the ExoMars LSS Breadboard 2 (LSS BB2) has been configured to have a mass of 114.5 kg. As not all sub-systems can be scaled down to an equivalent Martian gravity, the LSS BB2 features a turret allowing for the adjustment of the overall centre of mass (CoM) as

shown in Fig. 2.



Figure 2. ExoMars LSS Breadboard 2 in the RCET Testbed (RUAG Space, Zurich)

For the correlation exercise, the CoM of each sub-assembly as reported in Tab. 1 and the geometrical dimensions reported in Tab. 2 and 3 were used.

Table 1. LSS BB2 Centre of Mass – operational configuration\*

Centre of Mass	Location (x,y,z) [mm]	Mass [kg]
Rover Body	-6; 37; 851	46.31
Front Left Bogie	362; 516; -15	21.70
Front Right Bogie	362; -516; -15	21.70
Rear Transv. Bogie	-589; 3; 18	24.75

\*The analytical tool loads each part with the given mass and CoM and computes dynamically the bogie CoM as a function of the joints angles.

Table 2. LSS BB2 Bogie Pivot Location – operational configuration

Item	Location (x,y,z) [mm]
Rover Body	0; 0; 0
Front Left Bogie	360; 372; 60
Front Right Bogie	360; -372; 60
Rear Transv. Bogie	-396; 0; 130

Table 3. LSS BB2 Centre of Wheel Location – operational configuration

Item	Location (x,y,z) [mm]
Front Left Wheel (FL)	680; 600; -156
Front Right Wheel (FR)	680; -600; -156
Centre Left Wheel (CL)	40; 600; -156
Centre Right Wheel (CR)	40; -600; -156
Rear Left Wheel (RL)	-680; 600; -156
Rear Right Wheel (RR)	-680; -600; -156
Wheel diameter	250

### 3. TOOL DESCRIPTION

#### 3.1. Overview

The analytical tool allows loading different geometrical configuration from the database and adjusting the rover body CoM. The rover heading angle (*yaw*), slope angle and step shape obstacle height can be selected by the user for a given analysis as shown in Fig. 3.

For the deployment phase, the same sequence as used during the test program can be loaded and analysed.

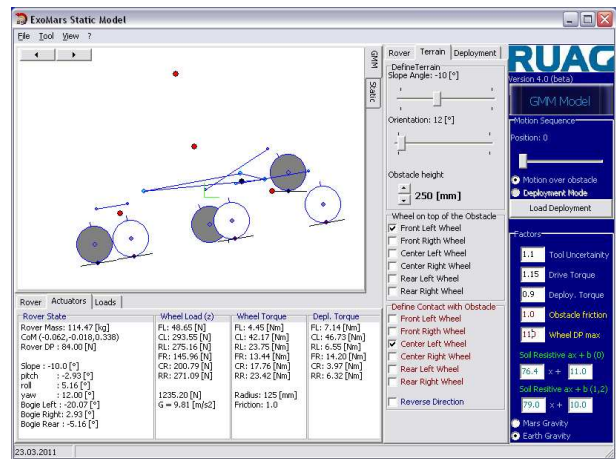


Figure 3. ExoMars LSS Analytical Tool user interface

For a given position or motion sequence, all loads are computed and displayed in real time in the graphical interface and in the panels. Detection of worst-case situation is performed based on a graphical analysis of a specific load (e.g. wheel, deployment or pivot) over all possible slopes and rover orientations. Sensitivity analysis can be performed by modifying a given dimension in real time and analysing the influence of it to a particular load case.

#### 3.2. Architecture

The tool solves the equation in a static way this mean without considering the history of the motion and in particular the inertia. This simplification allows calling the following functions one after the other:

- LSS Geometrical Model : computing the rover state based on the deployment joint angle and terrain slope
- LSS Placement Module: able to position the rover on obstacles such as all wheel are in contact with the terrain
- Wheel Load Computation: solving the Newton-Euler equation for determining the vertical load acting on each wheel
- Wheel Torque Computation : determining the wheel torque to be applied for a given motion
- LSS Motion Module: includes a wheel-soil

interaction model in order to determine if the motion can be successfully performed or not

- Deployment Torque Computation : determining the torque to be applied at the deployment joint
- Structure Load Computation : determining the forces and moments acting on the passive joint

For motion over an obstacle, various slope angle or deployment analyses, a pre-defined sequence is loaded and sent to the above modules in an iterative way.

The loads and torques determined by the tool can be exported and post processed with for example an actuator model in order to determine the electrical power consumption including ECSS factors.

### 3.3. External Interfaces

The tool can directly interface a database containing all LSS elements representing the latest version of each item composing the rover including their mass and centre of mass (CoM).

The tool is also able to load direct drive sequences used during the rover level test programme for the deployment and wheel-walking mode in csv format. By loading this input file, the analytical tool is able to simulate the deployment or wheel-walking sequence and allows direct comparison with the test data.

## 4. DESCRIPTION OF EACH FUNCTION

### 4.1. Geometrical Model

The geometrical model is constructed in a hierarchical manner starting with the rover body to which the 3 beams are attached, then the deployment units, the electronic box, the steering units, the drive units and finally the wheels. The visualisation of the geometrical model is given in Fig. 4 with the rotating joints appearing in blue and the centres of mass in red.

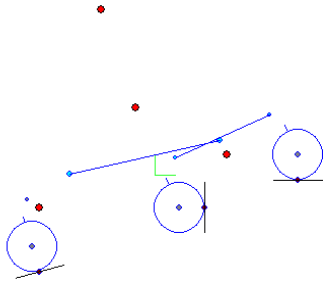


Figure 4. ExoMars LSS breadboard 2 geometry

This node based construction allows each sub-assembly to be described in its own coordinate system in terms of dimension and CoM in order to be compatible with a CAD model output. Moreover, this allows the user to

modify the geometrical dimension or CoM location of each part individually in order to perform a parametrical analysis.

A software vector library is then applied to rotate each sub-assembly in accordance with the rover's various degrees of freedom. This allows computing the rover's state and CoM as a function of the rover position and orientation (*pitch, roll, yaw*), the bogie and the deployment joint angles.

### 4.2. LSS Placement Module

The placement module is responsible of computing the rover orientation (*pitch, roll*) and bogie angles ( $\theta$ ) such that all wheels are in contact with the terrain. This is performed based on the heights ( $Z$ ) of the 6 wheels.

For an ExoMars rover suspension concept in operational configuration and with symmetrical bogies (i.e. pivot located in the middle of the wheels), the angles are determined with following equations in world coordinate system:

$$\theta_l (\text{left\_bogie}) = \arcsin \frac{Z_{cl} - Z_{fl}}{2b} \quad (1a)$$

$$\theta_r (\text{right\_bogie}) = \arcsin \frac{Z_{cr} - Z_{fr}}{2b} \quad (1b)$$

$$\theta_b (\text{rear\_bogie}) = \arcsin \frac{Z_{rl} - Z_{rr}}{w} \quad (1c)$$

$$\text{roll} = \arccos \frac{B}{\sqrt{A^2 + B^2}} - \arccos \frac{C}{\sqrt{A^2 + B^2}} \quad (2)$$

$$A = 2w; B = h \cdot (\cos \theta_l - \cos \theta_r)$$

$$C = \frac{1}{2} \cdot (Z_{fr} + Z_{cr} - Z_{fl} - Z_{cl})$$

$$\text{pitch} = \arccos \frac{B}{\sqrt{A^2 + B^2}} - \arccos \frac{C}{\sqrt{A^2 + B^2}} \quad (3)$$

$$A = P_x + L; B = P_z \cos(\text{roll}) - h_r \cos \theta_b$$

$$C = \frac{1}{2} \cdot (Z_{rr} + Z_{rl}) - Z_p$$

$Z$ : wheel height in  $z$  from the terrain [m]

$Z_p$ : middle of the front pivots height in  $z$  [m]. This can be computed based on the roll and front bogie angle.

$b$ : front bogie pivot to wheel centre in  $x$  [m]

$w$ : wheel track [m]

$h$ : front bogie pivot to wheel centre in  $z$  [m]

$h_r$ : rear bogie pivot to wheel centre in  $z$  [m]  
 $P_x$ : front bogie pivot location in  $x$  [m]  
 $P_z$ : front to rear bogie pivot distance in  $z$  [m]  
 $L$ : rear wheels distance in  $x$  [m]

Once the rover is placed on the obstacle, it can be positioned on every slope by rotating the overall rover to the given angle by adding the slope angle to the *pitch* and finally rotated around the terrain normal vector according to the heading angle *yaw*. This methodology allows analysing and producing a graphical output for a motion over a given obstacles on all required slopes and possible rover orientations for determining the worst case situation.

#### 4.3. Wheel Load Computation (without internal forces)

Once the rover is placed on the terrain, the wheel load is computed based on the CoM position of each mobile element and the wheel-soil contact points. Various approaches were implemented and compared with the test results. In order to have an accurate computation, the degree of freedom needs to be considered properly. Therefore the load computation outlined hereafter is specific to an ExoMars suspension and would need to be adapted for other rover concepts.

First the rover body mass is projected on each of the 3 bogies taking into account the front bogies degree of freedom. The force acting on the rear bogie ( $F_R$ ) is given in Eq. 4.

$$F_R = m_{body} \cdot g \cdot \frac{L_1}{L_1 + L_2} \quad (4)$$

$m_{body}$ : rover body mass [kg]  
 $L_1$ : body CoM distance to mean rear wheel contact points in  $x$  [m]  
 $L_2$ : body CoM distance to front pivot in  $x$  [m]

Based on the transverse bogie DoF, a similar methodology is used between the front left ( $FL$ ) and front right bogie ( $FR$ ) load distribution:

$$F_{FL} = m_{body} \cdot g \cdot \frac{L_2}{L_1 + L_2} \cdot \frac{W_1}{W_1 + W_2} \quad (5)$$

$W_1$ : body CoM distance to mean right wheel contact points in  $y$  [m]  
 $W_2$ : body CoM distance to mean left wheel contact points in  $y$  [m]

Then each bogie is solved separately with the same methodology by adding the bogie CoM to the rover body mass computed previously. In reality, a bogie could influence each other except on

the rotation axis but, due to the relatively long distance between the bogies and the limited slope angles, this effect is not significant and was neglected.

#### 4.4. Wheel Torque Computation (without internal forces)

For a six motorised wheeled rover, there are an infinite number of solutions that satisfy the Newton-Euler constraint (i.e. equilibrium). Overcoming this issue is not trivial and was explored at LSS level in [2] for a rover moving on a homogenous hard surface described with a unique friction coefficient.

In order to overcome such a limitation a wheel-soil interaction model working with various soils and obstacle needs to be implemented and a way of solving the equations at wheel level needs to be considered.

An obvious solution to the equilibrium is that each wheel is providing the torque necessary to counteract its own resistive forces. This methodology was investigated in this study.

Due to the selected architecture, the forces acting on the wheel are split in two categories: the resistive force due to the gravitational field and the resistive forces due to the wheel-soil interaction. The wheel torque  $T$  can therefore be described as

$$T_i = F_i \cdot x_i + R_i \cdot r \quad (6)$$

$F_i$ : wheel load in  $z$  direction [N]  
 $x_i$ : distance between the wheel centre and the contact point in  $x$  direction [m]  
 $R_i$ : sum of the wheel-soil interaction resistive forces [N]  
 $r$ : undeflected wheel radius [m]

Equation 6 was verified experimentally for a rover overcoming a step shape obstacle and provides accurate results for the sizing case, i.e. when a wheel is in front of a step shape obstacle and the other wheels are pushing against it as shown in Fig 5.

#### 4.5. Wheel Load Computation (with internal forces)

Even if the Eq. 6 is sufficient for sizing the actuators, this equation does not consider that the other wheels need to provide a normal force such as the wheel in front of the obstacle can move upward. This needs to be taken into account for determining accurately the power consumption at LSS level and is based on the following equation:

$$N_{\min} = \frac{F_i}{\mu} \quad (7)$$

$N_{\min}$ : Minimal normal force to be provided such as the wheel can overcome the load  $F$  acting on it [N]  
 $\mu$ : Wheel-obstacle friction coefficient to be determined experimentally

The LSS controller is commanding the wheel at a given speed and not in accordance with the minimal required torque necessary for overcoming an obstacle as given in Eq. 7. Therefore it is not necessarily the case that the other wheels will not provide a force  $N$  greater than the minimal required value.

In order to be independent from the control strategy, two boundary conditions were considered:

1. The wheels provide the minimum required tractive force such as the front wheel can move upward. The friction coefficient was determined experimentally by comparing the normal force and the wheel load.
2. The wheels provide the maximum possible tractive force that corresponds to the drawbar pull ( $DP$ ) at maximum allowed slip. This value was determined experimentally with a dedicated drawbar pull versus slip test program.

The first case is challenging to determine due to the fact that with multiple motorised wheels, an infinite number of solutions exist. For overcoming this mathematical issue and because this tool is focused on the sizing cases, the investigations were focused on the most difficult obstacles.

Based on the specification, the worst case situation is on a slope when a step shape rock is presented simultaneously on both sides such as two wheels have to overcome the obstacle. Therefore twice the force  $N$  has to be provided by the remaining four wheels.

The minimal corrective torque ( $T$ ) on those wheels is assumed to be proportional to the wheel load and the maximum value represents the wheel capability on a given soil:

$$r \cdot \frac{F_3}{\mu} \cdot \frac{F_1}{F_1 + F_2} < T_1 < r \cdot DP_1 \quad (8a)$$

$$r \cdot \frac{F_3}{\mu} \cdot \frac{F_2}{F_1 + F_2} < T_2 < r \cdot DP_2 \quad (8b)$$

$F_i$ : wheel load in  $z$  direction [N]

$DP_i$ : wheel drawbar pull capability at a given slip [N]

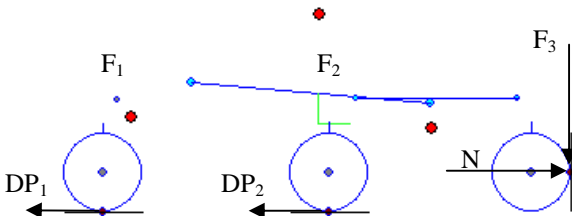


Figure 5. ExoMars LSS corrective torque for a double sided step shape obstacle

#### 4.6. LSS Motion Module

In order to determine if a motion can be performed, the nature of the soil and wheel-soil interaction parameters need to be considered. When the wheels in contact with the soil cannot provide a sufficient traction such as the other wheels can overcome an obstacles, the Eq 8 is not satisfied and the rover cannot perform this motion. This provides a success criterion that is used for sizing properly the LSS in order to meet the required motion capability.

In the case presented in Fig. 5, during a short time, the rover cannot move forward and as such the wheel 1 and 2 will have an extremely high slip i.e. 80 to 90%. The wheel drawbar pull value is determined experimentally at this slippage as a function of the soil and wheel load. Such input is used by the motion module in order to determine the rover motion capability and in order to compute the mechanical peak power consumption in this worst-case situation.

#### 4.7. Deployment Torque Computation

The deployment torque is less complex to compute because the actuators only have to overcome the gravitational load and the harness resistive torque. Assuming the wheels do not contribute to the deployment (i.e. worst-case situation), then the deployment torque  $T_{DEP}$  is given by:

$$T_{DEP,i} = F_i \cdot x_i + T_{harness} \quad (9)$$

$F_i$ : wheel load in  $z$  direction [N]

$x_i$ : distance between the deployment joint and the contact point in  $x$  direction [m]

$T_{harness}$ : harness resistive torque [Nm]

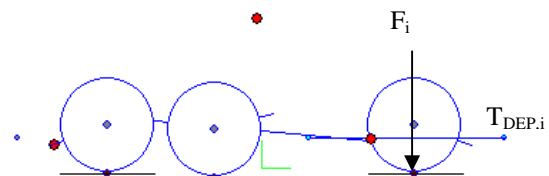


Figure 6. ExoMars LSS deployment torque

#### 5. CORRELATION

The equations presented in the previous chapter were implemented in the analytical tool and correlated with the test data produced during the ExoMars LSS phase B2X2 [3] as follow:

- Check that the CoM is computed correctly
- Compare the wheel load (static and dynamic)
- Compare the wheel torques during a motion over a step shape obstacle
- Compare the deployment torque on various slopes

### 5.1. CoM Verification

The first verification presented in Tab.4. is to compare the computed overall rover CoM (based on individual elements) with the measured one.

Table 4. CoM correlation

Value	LSS BB2	Tool	Offset
Mass	114.33 kg	114.47 kg	0.14 kg
CoM x	5 mm	8 mm	4 mm
CoM y	3 mm	16 mm	13 mm
CoM z	341mm	342 mm	1 mm

The prediction correlates accurately with the exception of the CoM in y direction. This is due to the asymmetrical accommodation of the F/T sensors not yet taken into account by the tool and that was corrected by shifting laterally the rover body CoM.

### 5.2. Wheel Load

The wheel loads correlation is performed based on the measured vertical forces acting on the wheel during a motion on soil ES-3 at both 0 and 40m/h as reported in Fig 7.

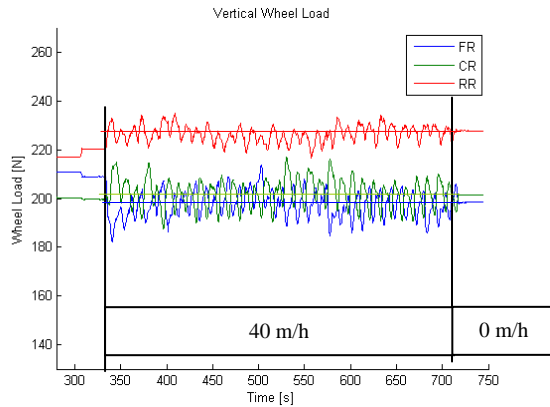


Figure 7. LSS BB2 wheel loads on ES-3

Table 5. Wheel load correlation – levelled surface

Wheel	Measured Value [N]	Analytical Value [N]	Offset [N]	Error [%]
FR(1)	204	180	24	12
FR(2)	179	180	-1	1
CR	197	178	19	10
RR	227	201	26	11
Total	123 kg	114 kg	-	-

The mean wheel load values recorded during the driving phase and the static wheel load values correlate with the prediction within 12%.

The sensor accuracy is 7.5% ( $\pm 15N$ ) and the front load recorded by the two different front right (FR) sensors shows a difference of  $\pm 12.5N$ . Moreover the sum of all sensors is 88N greater than the effective rover mass. By subtracting this sensor offset (i.e. 88/6 N), the difference with the predicted value is within 5%.

The dynamical load variation of 5% around the mean value visible on Fig. 7 is due to the grousers and needs to be taken into account for providing accurate dimensioning loads. Based on this correlation a correlation factor of 1.1 seems to be sufficient in order to cover both the tool accuracy of 5% and the dynamical effect of 5%. This factor was implemented in the analytical tool and can be modified if necessary by the user.

### 5.3. Wheel Torque

The wheel-soil resistive force ( $R_i$ ) used in Eq. 6 needs to be determined by a dedicated wheel-soil interaction module or experimentally in function of the soil and wheel load. The tests on soil ES3 presented in [3] have recorded a mean drive torque on levelled terrain at a given wheel load. Wheel level tests on the same soil performed by DLR Bremen with the ESA RCET facility [1] demonstrates that the resistive torque is sensitive to the multipass effect, to the wheel load but not to the rover speed. Based on the wheel level test data, the following relationship was found for an ExoMars flexible wheel on soil ES3 without multipass ( $R_0$ ) and with multipass ( $R_{i,2}$ ):

$$R_{i,0} = 0.0764 \cdot F_i + 11 \quad (10a)$$

$$R_{i,1or2} = 0.079 \cdot F_i + 10 \quad (10b)$$

The wheel peak torque correlation when moving over a step shape obstacle on both side simultaneously is reported in Tab.7 and Tab. 8.

Table 7. Wheel peak torque correlation – 25cm step shape obstacle both sided on ES3 from [3]

Wheel	Measured Value [Nm]	Analytical Value [Nm]	Error [%]
FR	24.1 ; 24.7 (21)*	20.9	14 (0)
CR	33.5 ; 36.7 (29)*	30.5	13 (5)
RR	30.1 ; 31.4 (29)*	29.1	5 (0)

\*Value in bracket represents a maximum of the mean values computed over 5 seconds (i.e. 25 consecutive data acquisition) in order to reduce the dynamical effects.

Table 8. Wheel peak torque correlation – 7cm step shape obstacle both side on ES3 for a 10° slope from [3]

Wheel	Measured Value [Nm]	Analytical Value [Nm]	Error [%]
FR	14.6 $\pm$ 1.2*	16.0	9.6
CR	28.0 $\pm$ 5.6*	30.5	8.9
RR	37.2 $\pm$ 2.2*	34.7	6.7

\*A deviation of the measured value is estimated based on 3 consecutive tests. The predicted value is within the reproducibility range.

The recorded peak torques correlate with the analytical tool within 14% on levelled surface or 5% if the maximum of the mean values is used and 10% on a 10° slope.

Based on the correlation exercise and using a similar approach than for the wheel load, we can estimate that the tool accuracy is within 10% and a dynamical effect of 5% needs to be taken into account for the wheel torque. To cover the above, a multiplication factor of 1.15 was implemented for the wheel torque computation in the analytical tool.

#### 5.4. Motion Capability

In order to define if the rover can overcome slopes or obstacles, the Eq. 8 is used with a drawbar pull capability at 80% slip corresponding to 90N per wheel. This value is based on wheel level test data performed by DLR but the slip value to be considered in a given situation is (TBC). Such values give a predicted slope gradeability on soil ES3 of 28°. The test indicates that 26° is very challenging. This difference is probably due to slip sinkage that is not taken into account by the tool and that increases the rover inclination of a couple of degree w.r.t the slope angle as recorded during the test campaign.

For wheel-rock interaction a friction coefficient of 1.0 was estimated by dividing the normal and tangential force recorded by the force sensors. With this value, an obstacle climbing is only possible with a drawbar pull value per wheel of at least 120N. Such a value seems not unrealistic if we consider that the wheel slip value in this particular situation can be momentary above 80%.

#### 5.5. Deployment Torque

The deployment torque is computed by the analytical tool using the same sequence of direct command as the breadboard.

Table 8. Deployment peak torque correlation – levelled surface with high friction coefficient

Depl.	Measured Value [Nm]	Analytical Value [Nm]	Error [%]
FR	39.1 ; 42.0 (+15)	62.7 (0)	54
CR	24.1 ; 13.7 (-)	14.6 (0)	23
RR	44.5 ; 48.0 (-)	54.3 (0)	17

Table 9. Deployment peak torque correlation – levelled surface on soil ES3

Depl.	Measured Value [Nm]	Analytical Value [Nm]	Error [%]
FR	48.6 (+8)	62.7 (0)	29
CR	13.4 (-)	14.6 (0)	9
RR	43.7 (-)	54.3 (0)	24

Table 10. Deployment peak torque correlation – 20° slope with high friction coefficient

Depl.	Measured Value [Nm]	Analytical Value [Nm]	Error [%]
FR	>80 ; 75 (+9)	119	53
CR	30 ; 20 (-)	28	12
RR	22 ; 23 (-)	28	24

In this case the predicted deployment torque is significantly higher than the measured values in particular for the front wheel that constitutes the sizing case. The error is similar for both deployments on 0° and 20° slope tending to indicate a permanent error in the prediction but a correct estimation of the slope influence.

One explanation of this effect is that the wheels that are not considered by the analytical tool during the deployment phase are helping more than expected. The driving torque is reported in bracket in the result tables and, as it can be seen when comparing a deployment on a hard surface (Tab. 8) and on loose soil (Tab. 9), the difference in the driving torque is equal to the delta in the deployment torque. I.e. considering wheel torque gives on hard soil a deployment torque of 40.5+15 Nm and on soil ES3 of 48.6+8 Nm. When comparing those values with the prediction, the correlation is within 13%.

There is no evidence that the wheel can always help during the deployment phase in particular because it depends on the friction coefficient and the synchronisation between the wheel and the deployment joint. Therefore the analytical tool is considered to provide a worst-case conservative estimation of the required sizing torque for the deployment unit and no additional multiplication factor need to be introduced.

#### 5.6. Power estimation

The required LSS mechanical power is given by the multiplication of the torque with the speed and as such is considered to be as accurate as the predicted torque value. This is justified by the fact that the actuators are close-loop controlled and no significant speed variations were observed between commanded and achieved speed during the test campaign.

The LSS electrical peak power estimation is a complex task requiring profound knowledge of the actuator flight model design including the thermal effect, harness and electronic losses. This estimation was performed using the mechanical power computed by the analytical tool but cannot be correlated with the LSS BB2 that is working at ambient and with standard actuators.

#### 6. FUTUR WORK

The ExoMars LSS analytical tool was developed in order to provide input to the sub-system in terms of sizing loads. Based on the promising results, different

enhancement could be envisaged:

- Integration of an LSS actuator model in order to have directly the LSS power consumption without having to post-process the data.
- Update of the placement module in order to be able to simulate asymmetrical deployment sequences and wheel-walking mode.
- Enhance the wheel-soil interaction module based on test data on other soils and obstacles.

A major future work could also be to interface the application with a 3D environment and develop a function capable of computing accurately the rover displacement in order to have full ExoMars motion simulation capability on Mars.

## 7. CONCLUSION

As a result of a test program conducted at both RUAG and DLR premises and previous simulation work reported in [1] and [2], the LSS team consolidated its understanding of the expected LSS behaviour on Martian representative terrain. This consolidation also included the effects of innovative developments like flexible wheels in interaction with loose soil and obstacles. The large volume of data coming from position sensors, force torque sensors and the actuators provided valuable information that was directly integrated in the analytical tool and used during the correlation exercise.

The ExoMars Locomotion Sub-system analytical tool is capable of assessing rover performances and providing relevant input for sizing the mechanical and electrical sub-system. The correlation exercise performed with the LSS Breadboard 2 demonstrates an overall prediction accuracy of 10% for the dimensioning driving cases on which an additional 5% needs to be considered for covering dynamic effects. For the deployment phase, the predicted deployment torque is always over estimated by a factor 1.2 to 1.5. This is mainly due to the fact that the tool is not considering the wheel contribution during the deployment. This effect is hardly predictable as it depends on the wheel-soil interaction and control aspect. However, when considering the measured wheel contribution, the prediction is overestimated by only 13%.

The proposed theoretical approach combined with a parametrical model allows rapidly exploring variations of the overall rover configuration, conducting sensitivity analysis and determining in an extremely short timeframe the worst case situations. Thanks to the tool accuracy and capability, a new LSS baseline capable of accommodating additional payload and larger wheels was selected. The tool prediction was used for sizing the sub-systems (e.g. actuators, pivot, suspension, wheel) and as inputs to the actuator model for computing the

required power and sizing the harness and electrical units.

The analytical tool relies on relatively simple equations and wheel level test data allowing straight forward implementation in any kind of software environment. Even if the equations presented in this paper are specific to an ExoMars type concept, the same approach could be applied to other passive suspension concepts. Due to its short development time, analytical capabilities and predictive accuracy, such a tool could be an alternative to more complex simulation applications in particular during the dimensioning phase, for selecting a baseline and in order to reduce power consumption, minimizing the sub-system masses and for optimizing the deployment sequence.

## 8. ACKNOWLEDGEMENTS

The work was performed in the context of a RUAG R&D activity for supporting planetary exploration rovers design. The adaptation of this tool presented in this papers was performed for supporting the ExoMars project within which RUAG is responsible for the Locomotion Subsystem, Astrium Ltd is responsible for the Rover Vehicle and Thales Alenia Space Italy is the overall mission prime contractor to ESA.

The authors would like to thanks the test engineers from DLR Institute of Robotics and Mechatronics, DLR Institute for Space Systems and ETH Zürich for the exceptional work performed within the test programme in terms of data acquisition and reporting.

The breadboard was developed by RUAG Space and BlueBotics. The breadboard control was developed by ETHZ.

## 9. REFERENCES

1. S. Michaud, L. Richter, T.Thueer, A. Gibbesch, T. Huelsing, N. Schmitz, S. Weiss, A. Krebs, N. Patel, L. Joudrier, R. Siegwart, B. Schäfer, A. Ellery, *Rover Chassis Evaluation and Design Optimization Using the RCET*, Proceeding of the ASTRA 2006, ESTEC, the Netherlands, 2006.
2. Krebs, T. Thueer, S. Michaud and R. Siegwart, *Performance Optimization of All-Terrain Robots: A 2D Quasi-Static Tool*, Proceedings of the International Conference on Intelligent Robots and Systems, 2006.
3. M. Apfelbeck, S. Kuß, B. Rebele, S. Michaud, C. Bösch, R. Krpoun, B. Schäfer, *ExoMars Phase B2 Breadboard Locomotion Sub-system Test Campaign*, Proceeding of the ASTRA 2011, ESTEC, the Netherlands, 2011.
4. S. Michaud, A. Gibbesch, T. Thueer, A. Krebs, C. Lee, B. Despont, B. Schäfer, R. Slade, *Development of the ExoMars Chassis and Locomotion Subsystem*, Proceeding of the I-SAIRAS 2008, JPL, Los Angeles, 2008.